Annu. Rev. Mater. Res. 2001. 31:291–321

DESIGN AND SYNTHESIS OF ENERGETIC MATERIALS[1]

Laurence E Fried, M Riad Manaa, Philip F Pagoria, and Randall L. Simpson
Energetic Materials Center, Chemistry and Materials Science Directorate, Lawrence Livermore National Laboratory, P. O. Box 808, Livermore, California 94551; e-mail: lfried@llnl.gov; manaa1@llnl.gov; pagoria1@llnl.gov; simpson5@llnl.gov

Key Words high explosive, heterocycles, high-energy density material, property prediction

■ **Abstract** Energetic materials are chemical compounds or mixtures that store significant quantities of energy. In this review, we explore recent approaches to property prediction and new material synthesis. We show how the successful design of new energetic materials with tailored properties is becoming a practical reality.

INTRODUCTION

Energetic materials include propellants, explosives, and pyrotechnics. These materials can be thought of as controllable storage systems for chemical energy. Propellants and pyrotechnics release their energy through relatively slow deflagration processes, often taking several seconds to achieve complete combustion. Explosives, on the other hand, release their energy on the microsecond timescale. Despite these differences, explosives, propellants, and pyrotechnics share several chemical similarities. In fact, explosive and propellant mixtures often share the same ingredients, although in different quantities. Energetic materials have numerous military and industrial applications. The vast majority of energetic materials are used by industry.

There is a continuing need for improved energetic materials. In developing new energetic systems, one seeks optimal tradeoffs in energy content, safety, and cost. This is achieved through formulation, that is, combining known chemical compounds, and/or synthesis, producing new compounds. There are significant

[1]The US Government has the right to retain a nonexclusive, royalty-free license in and to any copyright covering this paper.

costs associated with either of these activities. Therefore, it is desirable to try to reduce the amount of trial and error in new material development by predicting energetic material properties.

In this article, we will review current methods to predict energetic material properties. Because this is a very broad area, we focus on the topics of energy content prediction (commonly termed performance) and safety characteristics. An accurate assessment of these material characteristics can be helpful in screening new candidate materials. In the past, these characteristics were predicted with empirical rules and intuition. The development of molecular modeling techniques now makes it possible to predict many, but not all, relevant material properties through much more fundamental means.

To begin we review methods to predict the energy release of an energetic material. This is usually the first step taken in evaluating a target energetic material. In the second section, we examine methods to predict the stability of an energetic material, with particular emphasis on sensitivity to shock or impact. In the final section, we discuss recently synthesized energetic materials, focusing on heterocyclic ring molecules. This class of materials combines favorable material characteristics with interesting synthetic chemistry. A list of material name abbreviations for common energetic materials is given in Table 1. Explicit structures are provided for novel energetic materials.

TABLE 1 Acronyms and abbreviations used for high explosive materials

DATB	1,3-Diamino-2,4,-6-trinitrobenzene
DINGU	Dinitroglycourile
EDNA	Ethylenedinitramine
HMX	Octahydro-1,3,5,7-tetranitro-1,3,5,7-tetraazacine
HNB	Hexanitrobenzene
NG	Nitroglycerine
NTO	3-nitro-1,2,4-triazol-5-one
PETN	Pentaerythritol tetranitrate
RDX	Hexahydro-1,3,5-trinitro-1,3,5-triazine
TATB	1,3,5-triamino-2,4,6-trinitrobenzene
TETRYL	N-methyl-N,2,4,6-tetranitro Benzeneamine
TNA	2,4,6-trinitroaniline
TNAZ	1,3,3-trinitroazetidine
TNB	2,4,6-trinitrobenzene
TNT	2,4,6-trinitrotoluene

PREDICTION OF ENERGY RELEASE

The energy content of an energetic material often determines its practical utility. The useful energy content is determined by the anticipated release mechanism. Since detonation events occur on a microsecond timescale, any chemical reactions slower than this are not relevant when considering a detonation. Another way of looking at energy release mechanisms is through thermodynamic cycles. Detonation can be thought of as a cycle that transforms the un-reacted explosive into stable product molecules at the Chapman-Jouget state (C-J) (1). This is simply described as the slowest steady-shock state that conserves mass, momentum, and energy. Similarly, the deflagration of a propellant converts the un-reacted material into product molecules at constant enthalpy and pressure.

Understanding energy release in terms of thermodynamic cycles ignores the important question of the timescale of reaction. Nevertheless, chemical equilibrium is often nearly achieved when energetic materials react. This is a consequence of the high temperatures produced by such reactions (up to 6000 K). We begin our discussion by examining thermodynamic cycle theory as applied to high explosive detonation. This is a current research topic because high explosives produce detonation products at extreme pressures and temperatures: up to 40 GPa and 6000 K. Relatively little is known about material equations of state under these conditions. Nonetheless, shock experimentation on a wide range of materials has generated sufficient information to allow reasonably reliable thermodynamic modeling to proceed.

One of the attractive features of thermodynamic modeling is that it requires very little information regarding the un-reacted energetic material. The elemental composition, density, and heat of formation of the material are the only information needed. Because elemental composition is known once the material is specified, only density and heat of formation need be predicted.

Material performance depends strongly on density; for example, the detonation pressure is roughly proportional to the square of the density (1). It is very difficult to calculate the density of a molecular crystal (2). Thus the density determination is often the most uncertain step in the prediction of energy release. Density in energetic materials has traditionally been found through group additivity methods (3, 4). The newest methods (5) are of comparable accuracy to more advanced techniques based on intermolecular potentials (6–9). Further improvements in intermolecular potentials may improve the accuracy of atomistic prediction methods (10). The existence of multiple possible polymorphs of varying density but similar energy remains an unresolved difficulty (2).

The heat of formation of each compound in the gas phase can be calculated via quantum chemistry (11). Recent advances in density functional methods make it feasible to determine the heat of formation of large energetic molecules from first principles (12). The calculation of the solid lattice energy, however, is more difficult. Recent techniques relate the surface area of the isolated molecule and electrostatic potential surface to the lattice energy (13).

In spite of these uncertainties, the prediction of densities and heats of formation can yield insight into possible material performance. In Figure 1 we calculate the detonation velocity of several explosives in two different ways, with the Cheetah 1.40 thermochemical code using the BKWC (Backer-Kistiakowski-Wilson/Cheetah) product library (14) at full crystal density. In the first set of calculations, the calculated detonation velocity was based on the experimental heat of formation and density. In the second set, the calculated detonation velocity was based on the predicted density and heat of formation. Densities were predicted with the MOLPAK (molecular packing) program (7). MOLPAK systematically searches through common crystallographic space groups and finds the minimum energy packing of molecules given empirically derived interaction potentials for rigid molecules.

The gas phase heat of formation was calculated using Hartree-Fock theory corrected by group equivalents, a method that is usually accurate to within 4 kcal/mol. The lattice energy was calculated with the MOLPAK program. We see that although differences owing to the use of calculated material properties are apparent, the calculated values are of sufficient accuracy to correctly order the detonation velocity of the various materials. Direct comparison with experimental detonation velocities is not made in the plot because experimental data are available only at densities less than the full crystal.

Chapman-Jouget (C-J) detonation theory (1) implies that the performance of an explosive is determined by thermodynamic states—the C-J state and the connected adiabat. Thermochemical codes use thermodynamics to calculate these states and hence obtain a prediction of explosive performance. The allowed thermodynamic states behind a shock are intersections of the Rayleigh line (expressing conservation of mass and momentum), and the shock Hugoniot (expressing conservation of energy). The C-J theory states that a stable detonation occurs when the Rayleigh line is tangent to the shock Hugoniot.

This point of tangency can be determined, given that the equation of state $P = P(V, E)$ of the products is known. The chemical composition of the products changes with the thermodynamic state, thus thermochemical codes must simultaneously solve for state variables and chemical concentrations. This problem is relatively straightforward because the equation of state of the fluid and solid products is known.

One of the most difficult parts of this problem is accurately describing the equation of state of the fluid components. Despite its simplicity and lack of rigorous derivation, the Becker-Kistiakowski-Wilson (BKW) (15) equation of state (EOS) is used in many practical energetic material applications. There have been a number of different parameter sets proposed for the BKW EOS (16–19). Souers & Kury (20) have critically reviewed these equations of state by comparing their predictions to a database of detonation tests. They concluded that BKW EOS could not adequately model the detonation of a copper-lined cylindrical charge. The BKWC parameter set for the BKW EOS (14) partially overcomes this deficiency through more aggressive parameterization techniques. However, BKWC is not

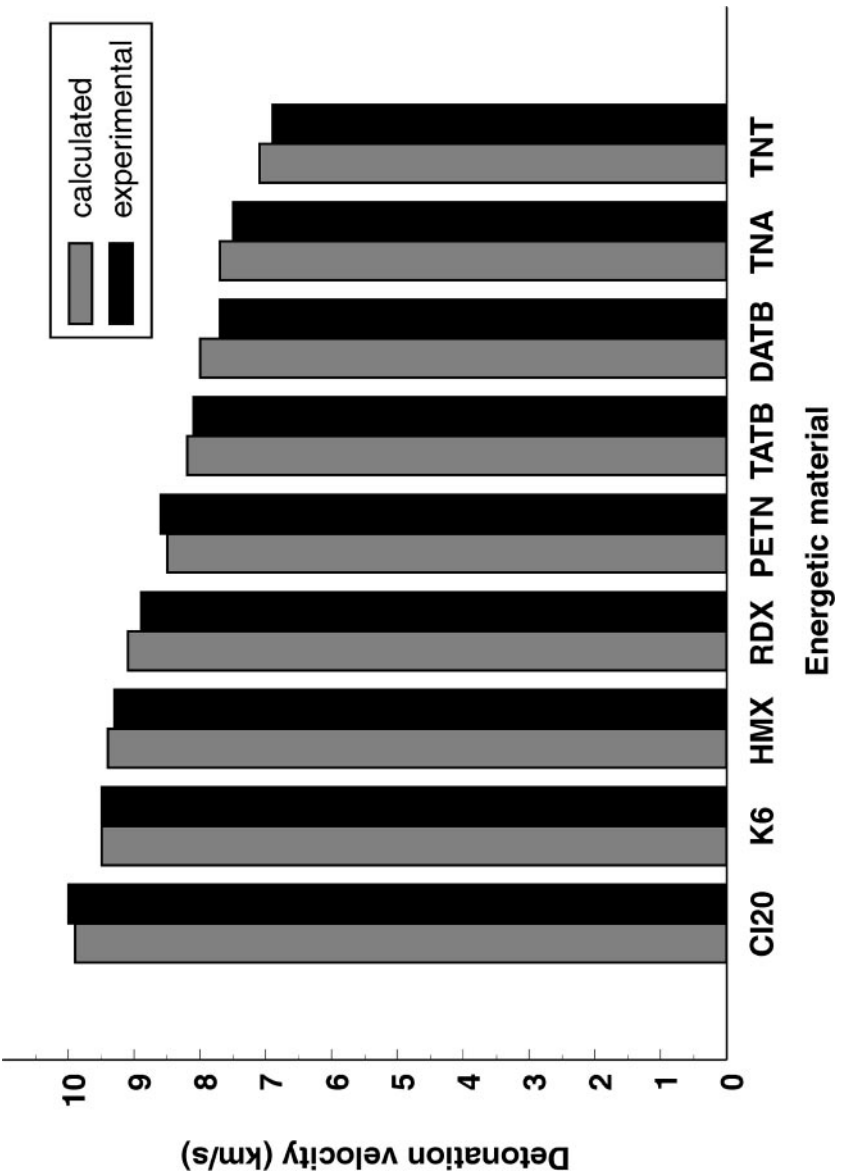

Figure 1 Detonation velocities predicted by Cheetah 1.40, based on calculated densities and heats of formation versus experimental densities and heats of formation.

reliable when applied to explosives very high in hydrogen content. It has long been recognized that the highly empirical nature of the BKW EOS limits the accuracy achievable in detonation calculations. This is particularly important when designing new materials that may have unusual elemental compositions. Efforts to achieve better EOS have largely been based on the concept of model potentials. With model potentials, molecules interact via idealized spherical pair potentials. Statistical mechanics is then employed to calculate the EOS of the interacting mixture of effective spherical particles. Most often, the exponential-6 potential is used for the pair interactions:

$$V(r) = \frac{\varepsilon}{\alpha - 6}[6\ \exp(\alpha - \alpha r/r_m) - \alpha(r_m/r)^6]$$

Here, r is the distance between particles, r_{m} is the minimum of the potential well, ε is the well depth, and α is the softness of the potential well.

The JCZ3 (Jacobs-Cowperthwaite-Zwisler/3) EOS was the first successful model based on a pair potential that was applied to detonation (21). This EOS was based on fitting Monte Carlo simulation data to an analytic functional form. Hobbs et al (22) recently reported a JCZ3 parameter set called JCZS (Jacobs-Cowperthwaite-Zwisler/Sandia). JCZS employs some of the parameterization techniques used in the construction of BKWC. It achieves better accuracy for the detonation of common high explosives than BKW EOS. Because JCZ3 is extensively parameterized to detonation, it has difficulty in reproducing reactive shock Hugoniots of hydrocarbons and other liquids (LE Fried, personal communication).

Ross proposed a soft-sphere perturbation theory for the EOS of the exponential-6 fluid (24). Ross, Ree, and others successfully applied this EOS to detonation and shock problems (25–28). Kang et al also derived a fluid perturbation theory designed to work at high density (29). Computational cost is a significant difficulty with an EOS based on fluid perturbation theory. Byers Brown (30) developed an analytic representation of Kang et al's EOS using Chebyshev polynomials. The accuracy of the above EOS has been recently evaluated (31); these authors conclude that Ross's approach is the most reliable. More recently, Fried & Howard have used a combination of integral equation theory and Monte Carlo simulations to generate a highly accurate EOS for the exponential-6 fluid (32).

The exponential-6 model is not well suited to molecules with a large dipole moment. Ree (33) has used a temperature-dependent well depth ε in the exponential-6 potential to model polar fluids and fluid phase separations. Fried & Howard have developed an effective cluster model for the HF (hydrogen fluoride) molecule (34) that is valid to lower temperatures than the variable well-depth model but employs two more adjustable parameters. More progress needs to be made in the treatment of polar detonation product molecules.

Efforts have been made to develop EOS for detonation products based on direct Monte Carlo simulations instead of analytical approaches (35). This approach is promising given recent increases in computational capabilities. One of the greatest advantages of direct simulation is the ability to go beyond van der Waals 1-fluid

theory (36). Kerley has advocated the ideal mixing approximation as an alternative to 1-fluid theory (37).

In most cases, interactions between unlike molecules are treated with Lorentz-Berthelot combination rules (38). Non-additive pair interactions have been used for N_2 and O_2 (28). The resulting model for N_2 accurately matches double-shock data, but it is not accurate at lower temperatures and densities (32). A combination of experiments on mixtures and theoretical developments is needed to develop reliable unlike-pair interaction potentials.

Many materials produce large quantities of solid products upon detonation, the most common of which is carbon, although some explosives produce aluminum and aluminum oxide (39). Uncertainties in the EOS and phase diagram of carbon remain a major issue in the thermochemical modeling of detonation. van Thiel & Ree have proposed an accurate Mie-Gruneisen EOS for carbon (40). Fried & Howard (41) have developed a simple modified Murnaghan EOS for carbon that matches recent experimental data on the melting line of graphite. There is considerable uncertainty regarding the melting line of diamond. Fried & Howard argue, based on re-analysis of shock data, that the melting line of diamond should have a greater slope. Shaw & Johnson have derived a model for carbon clustering in detonation (42). Viecelli & Ree have derived a carbon-clustering model for use in hydrodynamic calculations (43, 44).

Thermochemical equilibrium is a first approximation to the chemical kinetic processes controlling detonation. We call an explosive ideal when thermochemical equilibration is nearly achieved in the detonation.We call an explosion non-ideal if the chemical kinetic processes in the detonation wave are poorly approximated by the thermochemical equilibrium, i.e., the chemistry is slower than the hydrodynamics. For most purposes, we define non-ideal explosives as those with a reaction zone of one millimeter or more. These materials have chemical reaction rates that are slow compared with a hydrodynamic time-scale (10^{-6} s) so that the C-J assumption of instantaneous thermodynamic equilibrium breaks down. For example, it is found experimentally that the detonation velocity of non-ideal explosives varies sharply from the C-J value and depends strongly on the cylindrical charge radius.

We are therefore forced to consider the interaction of chemical kinetics with the detonation wave in order to reach an acceptable representation of detonation in non-ideal explosives. Wood & Kirkwood (WK) (45) proposed a two-dimensional steady-state kinetic detonation theory that solves many of the limitations of ZND (Zeldovich-von Neumann-Doring) theory. ZND theory treats a two-dimensional detonation wave. It predicts a high-pressure precursor to the C-J state known as the von Neumann spike (1). WK theory considers a cylindrical charge of infinite length. It solves the hydrodynamic Euler equations in the steady-state limit along the central streamline of the cylinder. Radial expansion is treated as a source term in the one-dimensional flow along the streamline. Bdzil has generalized WK theory to off-axis flow (46). Stewart (47) and co-workers have studied the effect of kinetic rates on the decrease of detonation velocity with decreasing size and on curvature of the detonation wave.

Howard et al (48) have implemented a model of detonation kinetics based on the identification of individual chemical species. The advantage of their treatment is that the same EOS and chemical rate laws can be used on a wide range of explosive mixtures. A mixture of EOS based on thermal, mechanical, and partial chemical equilibrium is used, as implemented in the Cheetah 2.0 thermochemical code (49). Small molecules that are gases at standard conditions are treated with the BKW EOS (14). This framework has been recently extended to the HMSA/MC (hypernetted mean spherical approximation/ Monte Carlo) EOS (32). Solids are treated with a Murnaghan (50) EOS, whereas chemical reaction rates, which depend only on pressure, are employed. These rates represent the consumption of the energetic material by the detonation wave. Fast reaction rates (partial chemical equilibrium) are assumed for species other than the initial material.

Howard, Fried, and Souers solved the WK equations numerically to find the steady-state detonation velocity. The radial expansion is derived from measured radii of curvature for the materials studied. They found good agreement with measured detonation velocities using the same set of EOS and rate laws for each composite. Although the treatment of detonation is by no means exact, the ability to model a wide range of phenomena based on simple EOS and rate laws is encouraging.

PREDICTION OF MATERIAL STABILITY

An energetic material may undergo chemical reaction in response to shock, thermal, or chemical insults. In this review, we concentrate on stability to shock excitation. It is often the case, however, that a material's stability to various forms of loading is highly correlated with one another. Energetic materials exist in a higher energy state than their lowest energy decomposition products. Thus energetic molecules are often termed metastable. Kinetic stability, however, guarantees that decomposition is sufficiently slow at ambient conditions that the species are long lived. Recently, several metastable nitrogen and oxygen compounds have been proposed that contain novel bonding. This has led to recent theoretical studies of hypothetical systems as high-energy density materials (HEDM), such as oxygen ring–strained systems (O_4 and O_8) (51, 52), tetrahedral N_4 (53), and cubic N_8 (54).

From a molecular perspective, the kinetic stability entails two presuppositions. The first is adiabatic stability. Energetic systems must exist at a metastable local minimum on the ground electronic state potential energy surface as a function of nuclear positions. There are significant energy barriers hindering decomposition on this surface. Second, a less commonly realized phenomenon concerns nonadiabatic stability, where processes involving excited electronic states are involved in the decomposition process.

The initial response of energetic molecular systems to shock or impact is a topic of considerable interest and controversy. The goal is to build predictive models

identifying molecular parameters that can be correlated with sensitivity and performance measures of the energetic molecule. Multiple parameters can be found that correlate with, but do not necessarily cause, energetic material sensitivity (55). Several mechanisms have been proposed that consider either molecular deformations or electronic excitations as the first event under high-pressure conditions.

Microscopic Models of Initiation

Understanding the first step in the response of energetic molecules to a shock is a topic of considerable importance because it ultimately would shed light on the sensitivity properties of energetic materials. It is known that the mechanical energy from compression leads to chemical decomposition and heating. Which bond in the molecule breaks first and what type of chemical reactions (unimolecular versus bimolecular, etc) occur first are still largely unknown, even for the simplest and widely studied systems such as nitromethane. Recent applications of ultrafast spectroscopic methods (56), however, hold great promise for understanding these basic mechanisms at the molecular level through direct spectroscopic measurements.

Several models have been proposed for the initial response of energetic molecular solids to instantaneous high pressure. The vibrational energy up-pumping model (57) suggests that the shock wave produces a bath of excited phonons absorbed by the lowest molecular vibrational modes. Increased phonon absorption and intramolecular vibrational energy redistribution (IVR) lead to excitation of higher-frequency modes. The molecule eventually reaches a transition state and proceeds to chemical reactions. Fried & Ruggiero (58) derived a simple formula for the total energy transfer rate into a given vibron band in terms of the density of vibrational states and the vibron-phonon coupling. The phonon up-conversion rates, based on small anharmonic terms in the Hamiltonian, were shown to correlate with the sensitivity in such explosives as TATB, HMX, and lead styphnate. Coffey (59) postulated that the process of initiation of chemical reactions is the result of tunneling of dislocations in a solid that, at high velocities, could have sufficient energies to directly pump the internal vibrational modes of the explosive molecules.

Other workers considered models associated with the electronic properties. Williams (60) was the first to examine the influence of electronic excited states and electronic transport on the initiation and propagation of detonation waves in solid explosives. He proposed initiation by changes in the Fermi level of solid explosives owing to a double electron and positive hole injection followed by chemical reactions. Dremin et al (61), noting evidence for similarities between shock decomposition intermediates to those of photochemical processes, proposed electronic excitation as the first molecular response in their multiprocess detonation model. Delpuech et al (62) proposed that the minimum polarity affecting an electronically excited state is a unique molecular parameter directly correlated within each family of organic explosives with shock sensitivity. Sharma reported the

existence of linear correlation between impact and shock sensitivity with electronic levels, the shake-up promotion energy observed in X-ray photoelectron spectra, of a homologous series of explosive compounds (63, 64). More recently, Gilman (65) postulated that the compression from the wave front causes local metallization, for instance, when bending of covalent bonds decreases the HOMO-LUMO (highest occupied molecular orbital–lowest occupied molecular orbital) gap.

With the aid of ab initio electronic structure calculations on the common explosive, RDX ($C_3H_6N_6O_6$), Kunz and co-workers proposed a mechanism based on electronic excitations induced by an impact wave propagating through the crystal (66). They showed that edge dislocations cause a dramatic reduction of the optical gap owing to the splitting of local electronic states from both the valence and conduction bands. The band gap is further reduced to near zero by the pressure inside the impact wavefront, resulting in the breakage of the N-NO_2 molecular bond.

Conclusive experimental evidence is still lacking in support of any of the models described above. The complexity of the process under shock or impact for solid materials is, at best, a multiscale event in time and space. Intuitively, electronic excitation is plausible, considering the fact that electrons are light, fast, and quantal, thus responding first to exterior perturbations. Following electronic excitation, however, several processes, including dissociation on the excited state surface, radiative processes, and nonradiative energy deactivation, could be at play to induce chemical reactions.

In a recent study, Manaa & Fried (67) have considered the topology of the ground and first excited states of nitromethane, a widely studied prototypical model of energetic materials. The equilibrium geometry of the triplet state of

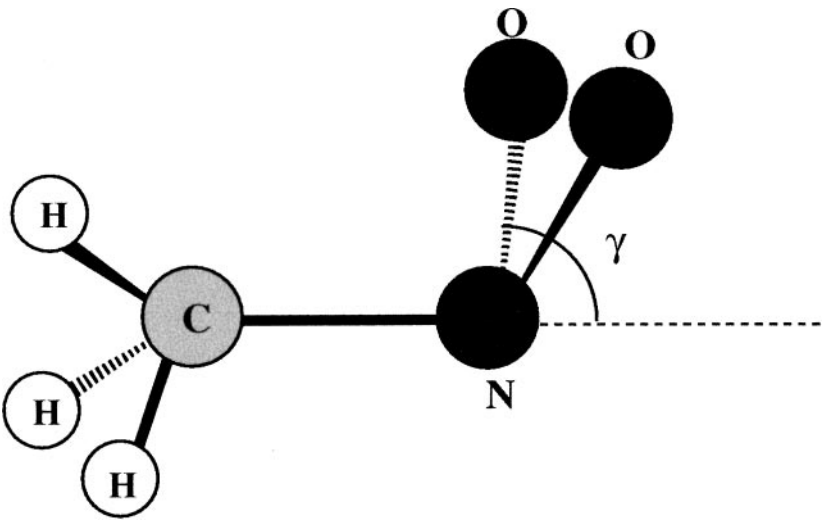

Figure 2 Geometric structure of nitromethane molecule at the equilibrium of the excited triplet state.

nitromethane is such that the ONO bond makes an angle of about 50° relative to the C-N bond (Figure 2), which is markedly different from the equilibrium geometry of the ground state where δ is zero. An adiabatic barrier to dissociation on this first excited state with respect to the C-N bond (see Figure 3) was determined (using highly correlated ab initio multireference configuration interaction methodology) to be about 33 kcal/mol. The existence of this barrier should presumably allow the triplet state to support a few vibrational levels and, owing to a different spin multiplicity that forbids decaying, to be long lived. An intersystem crossing, however, provides a nonradiative deactivation channel. Such a crossing has been located by determining the minimum energy crossing point (MECP) on the singlet-triplet surface of intersection. This point, as indicated in Figure 3, is located 13 kcal/mol above the equilibrium geometry of the triplet state, thus establishing a second barrier for energy redistribution that is more than half of the adiabatic one. It is expected, therefore, that thermal activation along the nitro-bending mode permits efficient energy transfer from the triplet state to higher vibrational levels of the ground surface. There are no experimental measurements on the triplet formation for nitromethane. Nevertheless, a recent study on nitrobenzene (68) showed that the triplet formation is very efficient with a quantum yield of $\geq$80% and that this state has a lifetime of $\leq$500 ps. An earlier study (69) established a short nonradiative lifetime of about 1 ps for the excited singlet state of nitromethane, with efficiency of 76% in energy deactivation. Vibrationally hot ground-state molecules could thus be generated by fast internal conversion (singlet-singlet) and intersystem (singlet-triplet) crossings. The excess nonradiative (kinetic: heat) energy could then be supplied to near shell molecules and speed up the decomposition process.

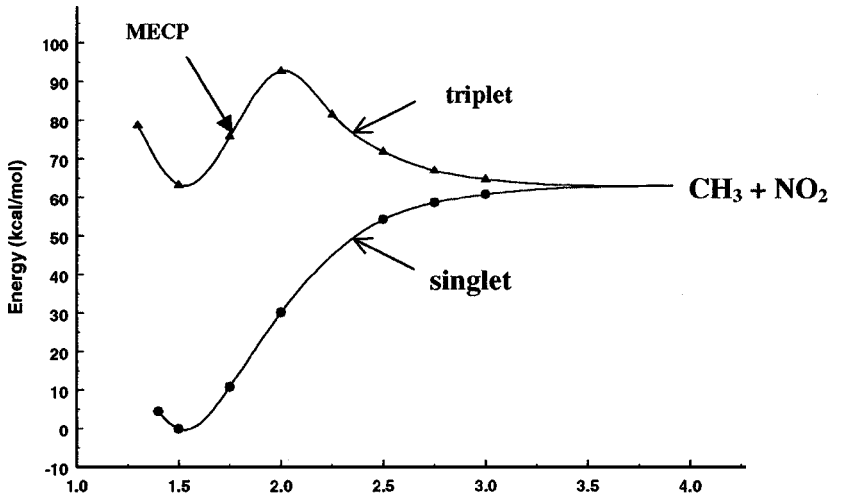

Figure 3 The optimized potential energy curves for the ground singlet and the excited triplet states of nitromethane.

Reed et al (70) have studied electronic excitations in solid crystalline nitromethane under conditions of shock loading and static compression. Bandgap lowering under uniaxial strain owing to molecular defects and vacancies was considered. Ab initio molecular dynamics simulations were done of all possible nearest neighbor collisions at a shock front and of crystal shearing along a sterically hindered slip plane. In all cases, the bandgap lowering was not sufficient to produce a significant population of excited states in the crystal.

The reaction chemistry under detonation conditions for most explosives, including materials as simple as diatomic nitric oxide, NO, is still largely unknown. The most widely studied example is nitromethane, a clear liquid with a density of 1.13 g/cm^3 at 298 K. Static high-pressure experiments (71, 72) show that the time of explosion for deuterated nitromethane is approximately ten times longer than that for protonated materials, suggesting that a proton or hydrogen atom abstraction is involved in the rate-determining step. Isotope-exchange experiments, using diamond cell methods, also give evidence (73) that the aci ion ($H_2CNO_2^-$) concentration increases with increased pressure. Other studies (74, 75) also suggest that reactions occur more rapidly and are pressure enhanced when small amounts of bases are present, giving further support to the aci ion production. Shock wave studies of the reaction chemistry are still inconclusive and at odds with mass spectroscopic studies. Mass spectroscopic studies suggested condensation reactions (76); time-resolved Raman spectroscopy pointed to a biomolecular mechanism (77); UV-visible absorption spectroscopy indicated either no sign of chemical reaction (78) or the production of $H_3CNO_2^-$ intermediate for amine-sensitized nitromethane (79). It was noted, however, that part of the discrepancy might be due to the fact that the ring-up (multiple shock) experiments are mapping lower temperature regimes (~1000 K) than experienced under detonation (76).

Molecular dynamics studies, using semi-empirical or preferably ab initio potentials for the molecular forces play an important role, at least in elucidating the initial steps of reaction mechanism. In the case of nitromethane, a preliminary fully ab initio molecular dynamics simulation was conducted recently (MR Manaa, manuscript in preparation). The calculation employed constant volume and temperature conditions similar to the C-J of fully reacted materials (density of 1.5 g/cm^3 and temperature of 3000 K). The initial step in the chemical reaction appears after 200 fs. As is shown in Figure 4, this first step is clearly identified with the hydrogen abstraction, and thus with the formation of aci ion, in accordance with experimental work noted above. This bond specificity is remarkable because in the gas phase, the C-N bond is the weakest, whereas the C-H bond is the strongest in the nitromethane molecule. In the condensed phase, however, vibrational energy is most significant in the C-H mode, in part owing to a caging effect that eventually leads to a proton extraction. Later snapshots of this simulation show that the proton transfers to an oxygen atom of a nearby nitromethane molecule. Similar simulations can be useful for characterizing the

first events in the decomposition process, although the molecular size might still hinder such undertaking.

Because of the extended time of the reaction zone of explosive materials (10^{-9}–10^{-6} s), ab initio methods are cumbersome and perhaps unrealistic for use in exploring decomposition kinetics. However, semi-empirical methods, such as tight-binding and bond-order type calculations, now offer a more realistic alternative, as recent simulations of shocked hydrocarbon materials indicate (80, 81). These methods can, in principle, be used for such extended times when implemented on massively parallel computer platforms.

The dissociation energy of the weakest bond of the explosive molecule is thought to play an important role in initiation events. However, previous attempts to correlate bond strengths to impact sensitivity were not successful (82). Politzer & Murray have calculated C-NO_2 and N-NO_2 bond dissociation energies in several small and moderately sized high explosives. They concluded that the correlation between bond strength and impact sensitivity is not general but limited within certain classes of molecules (82).

Given the complexity of detonation chemistry of high explosives, it is not surprising that bond dissociation energy alone is not enough to capture high explosive sensitivity. In order to understand this phenomenon, we herein examine the energy content of high explosives. Wu & Fried (83) have shown that the bond dissociation energy scaled by energy content is a promising indicator for predicting high explosive sensitivity.

We have listed the the calculated (using density functional methods) strengths of the weakest bond (N-NO_2 or C-NO_2) in Table 2. Impact sensitivity is usually characterized through a drop hammer test. In this simple experiment, a weight is dropped on the explosive from varying heights. The height at which violent reaction occurs 50% of the time is referred to as the drop hammer height (H_{50}) The impact sensitivity measurements are taken from the *LLNL Explosives Handbook* (84), the *Navy Explosives Handbook* (85), and Kohler & Meyer (86). Note that these types of measurements are typically rough. Measured impact sensitivities depend strongly on the apparatus used and the experimental protocol.

There appears to be some relation between the bond dissociation energy D_e and explosive sensitivity, but it is clearly not the only controlling factor. For instance, HNB is the most sensitive material in the comparison study, but has a D_e value similar to the much less sensitive DINGU. Nitrobenzene compounds, which are the least sensitive compounds studied here, are found to have the highest D_e values.

It is clear that the energy content of the material must also play a role in determining the impact sensitivity. It is well known that high-energy materials tend to be more sensitive. We have determined the energy content of the explosives studied here with the Cheetah 2.0 thermochemical code (49). The Cheetah code is used to determine E_d, the energy of decomposition, into equilibrium products at standard state, which is a measure of the total energy content of the material. We

TABLE 2 Bond strength (D_e) of the weakest bond, energy content (E_d, kJ/cc) and impact sensitivity H_{50} (cm) of high explosives

Material	Weakest bond	D_e (kJ/mol)	E_d (kj/cc)	H_{50} (cm)
TATB	C-NO_2	323	8.6	>320
DATB	C-NO_2	312	8.6	>320
TNA	C-NO_2	300	8.1	177(N)[a]
NTO	C-NO_2	284	7.7	>280
TNB	C-NO_2	283	8.6	100(N)[a]
TNT	C-NO_2	261	7.7	148
EDNA	N-NO_2	207	9.2	35 (K)[b]
HNB	C-NO_2	183	14.3	8.5
DINGU	N-NO_2	180	8.5	24 (K)[b]
HMX	N-NO_2	179	11.1	32
RDX	N-NO_2	174	10.4	28
TNAZ	C-NO_2	167	11.2	29
PETN	O-NO_2	167	10.5	14
NG	N-NO_2	157	10.0	20
TETRYL	N-NO_2	120	8.8	37

[a](N) indicates values from the *Navy Explosives Handbook* (85).

[b](K) indicates values from Kohler & Meyer (86).

All other data were taken from LLNL measurements.

display the results of these calculations in Table 2. Energy content can be used to explain some of the apparent anomalies in the D_e results. For instance, although HNB has a typical D_e value, it has the greatest energy content.

In Figure 5 we show scatter plots to help visualize the results of Table 2. Note that a logarithmic axis is used to represent the drop hammer values (H_{50}). D_e is seen to be useful in separating the very insensitive materials such as TATB, DATB, TNA, and NTO. Within the group of more sensitive materials, however, there seems to be little apparent relation between D_e and H_{50}. The opposite conclusion appears to be true of the energy of decomposition E_d. The relationship between E_d and impact sensitivity appears to be strongest for materials that are very high in energy and becomes more constant at larger H_{50} values.

The ratio between D_e and E_d could be an important quantity in determining the impact sensitivity. The physical motivation for this is that D_e plays the role of an activation barrier. Once a microscopic region ignites in response to mechanical deformation, E_d controls the energy released by the reaction. This in turn will control the local temperature and the likelihood of a propagating chemical reaction.

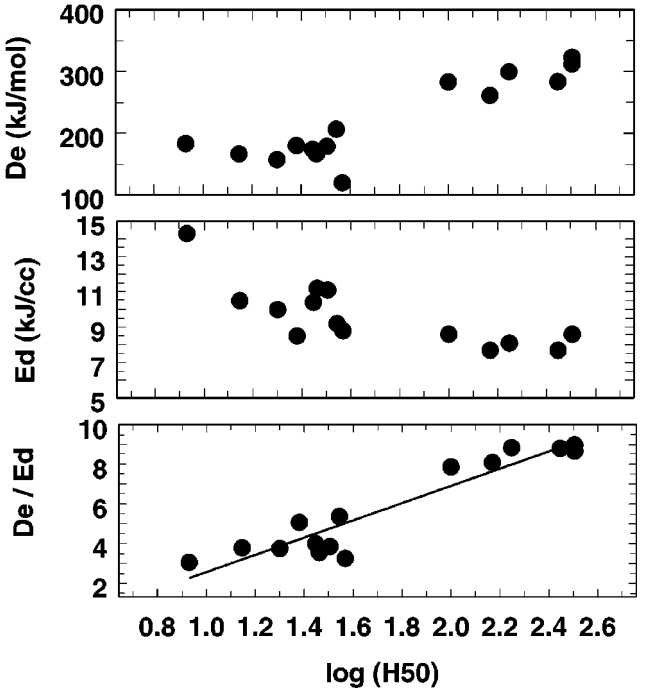

Figure 5 Bond dissociation energies (D_e), Decomposition energies (E_d) and the ratio D_e/E_d are plotted versus the log of the drop hammer height.

Arrhenius kinetics depends on the ratio of activation barrier to temperature, thus motivating the observed correlation between D_e/E_d and H_{50}.

High-Energy Density Materials: Polynitrogen

In contrast to the same group elements (phosphorus and arsenic), nitrogen has thus far resisted transformation from its basic molecular diatomic phase. The possible existence of polymeric forms of nitrogen, in which the strong triple bond of the diatom is replaced by single or single and double bonds, is of a particular interest because of the energetic properties associated with these materials. As potential high-energy density materials from an abundant natural source, they become leading candidates for high-energy density materials. To date, the only known forms of nitrogen are N_2 and N_3^-. Recently, the synthesis of the ion N_5^+ (C_2v symmetry) in a complex with AsF_6 anion (87) is an encouraging step toward the realization of these materials.

The prospect of destabilizing the strong N≡N triple bond under high pressure invited several experimental (88, 89) and theoretical (90–92) attempts to locate and

characterize bulk polymeric phases. Hemley et al (89a) have recent papers showing evidence for a polymeric phase. Calculations suggest polymeric regimes to exist below 100 GPa, at 70 and 50 GPa, whereas diamond-anvil-cell experiments failed to record a transition from the diatomic form for pressures of up to 180 GPa. In a non-static, shock-compressed nitrogen experiment (93) an anomaly at pressure above 30 GPa was recorded that was later interpreted as a dissociation to dense atomic phase (94).

Quantum chemical-based computational studies at various levels of theory (53, 54, 95, 96) have shown that N_4 and N_8 are metastable species, having (several) local minima on their respective potential energy surfaces. For tetrahedral N_4 (Figure 6*a*), Lee & Rice determined (53) the energy difference ΔE ($N_4 - 2N_2$) to be 778 kJ/mol and calculated an energy barrier to decomposition of 255 kJ/mol. Later work examined reaction pathways to other structures (95) and determined the lowest-energy conformation of N_4 to be an open-chain triplet (97) and a dissociation barrier of 264 kJ/mol (98). The results suggest that tetrahedral N_4 has a reasonably long lifetime and can be trapped and studied by matrix isolation techniques.

Computational studies on polyazacubane (99, 100) indicate that the high-energy content of these species, ΔE ($N_8 - 4N_2$) $=$ 1770 kJ/mol for cubic N_8 (Figure 6*b*), is not the result of strain energy but rather of a weak N-N single bond. Five isomers of N_8 have also been predicted to be metastable (96, 101), using highly correlated methods. In order to guide laboratory synthesis, protonated structures of N_4 and N_8 have been optimized and harmonic vibrational frequencies calculated (102). Recent studies reported ten isomers of N_8 corresponding to analogous CH

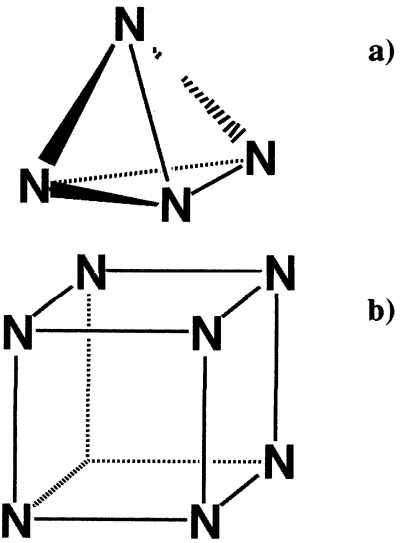

Figure 6 (*a*) Tetrahedral N_4 and (*b*) cubic N_8.

structures (103) and the isomerization reaction of N_8 cubane to planar bicyclic (pentalene-like) structure.

Recently (104), these provocative ideas were suggested: (*a*) Could a nitrogen fullerene analog, N_{60}, be a possible candidate, and (*b*) if so, what is a reasonable building block for such a cluster. In this vein, several computational methods were employed to locate extrema of bicyclic N_{10}. A geometry search located a planar structure (D_2h symmetry) as a saddle point and an orthogonal structure (D_2d symmetry) as a local minimum, with only 13–25 kJ/mol separating the two structures. The equilibrium structure was determined to be remarkably stable with respect to ring-connecting bond homolysis. Furthermore, it was postulated that this molecule could serve as a building block for yet a super-high-energy content N_{60} cluster, which was shown to have a local minimum with purely single-bonded nitrogen atoms. Harmonic vibrational frequencies of N_{10} and infrared active modes of N_{60} were reported to aid in future identification of these species.

For nitrogen, one triple bond is stronger than three single bonds, whereas for carbon the opposite is true. This is perhaps why nitrogen analogs of conjugated carbons are yet to be discovered. Computational tools are currently efficient, however, and should eventually indicate if there is a viable pathway for the experimental characterization and production of some form of polymeric nitrogen.

SYNTHESIS OF NOVEL ENERGETIC MATERIALS

In recent years, the synthesis of energetic heterocyclic compounds has received a great deal of interest. Heterocycles generally have a higher density and oxygen balance, important parameters for increasing the performance of an energetic material, than their carbocyclic analogues. Heterocycles high in nitrogen content also tend to have high heats of reaction. In this review, we discuss recent advances in the synthesis of heterocycles as energetic materials. Other types of novel energetic materials have been reviewed by Agrawal (105).

Pyrazoles

Molecular modeling and thermochemical codes have been used to guide the synthesis of new energetic materials containing the pyrazole ring. This is one of the few examples in which molecules were designed with modern tools, synthesized, and characterized. Caged molecular compounds and fused ring systems typically have higher densities than their single-ring analogues. For this reason, we investigated several fused ring systems computationally. Density predictions were made with the MOLPAK program, whereas predictions of heats of formation were based on Hartree-Fock calculations in combination with empirical corrections calibrated to energetic and non-energetic materials.

It was found that ring systems containing two fused 5-member rings consistently yielded higher densities than two fused 6-member or 4-member rings. The ring

TABLE 3 Predicted densities and heats of formation for target energetic materials

Material	Density[a] (g/cc)	Density[b] (g/cc)	Heat of formation[c]	Heat of formation[d]
DNPP	2.0	1.9	339	287
LLM-119	1.9	2.0	510	584
LLM-121	2.2	2.0		500

[a]MOLPAK 1 computer program used.

[b]Group additivity method of Ammon & Mitchell.

[c]Corrected Hartree-Fock calculations.

[d]DFT calculations (P. Politzer, private communication).

systems chosen for synthesis were predicted to be flat, thus enhancing packing. We also chose heterocyclic ring molecules as a way of improving the energy content of the molecule. Unsaturated bonds in the ring system also improved the calculated energy content and density. Densities and heats of formations were predicted for the target materials by several methods. The results of these calculations are shown in Table 3. Version 1 of the MOLPAK density prediction code was used because potential parameters used in more recent versions were not available for fused heterocyclic ring systems.

In Figure 7, we show pyrazoles that were developed at Lawrence Livermore National Laboratory. Energy release from the C-J state is a more reliable indicator of detonation performance than the detonation velocity. The energy release at a relative volume expansion of 2.2 is a good indicator of the energy usable for rapid metal acceleration. Based on the MOLPAK densities and Hartree-Fock heats of formation shown in Table 3, the metal acceleration energy of three compounds—DNPP, LLM-119, and LLM-121—were predicted to be 0.95, 1.1, and 1.4 times that of HMX, respectively.

Efforts to synthesize these materials began with 3,6-dinitropyrazolo [4,3-c]pyrazole (DNPP). In 1993, Shevelev and co-workers (106) reported its synthesis. Pagoria et al (107) developed an alternative synthesis of DNPP that eliminated the need for an extraction step, thus making the synthesis more amenable to scale-up. DNPP has a measured ΔH_f of +272 kJ/mol, in good agreement with the simple Hartree-Fock calculation in Table 3. The crystal density was determined

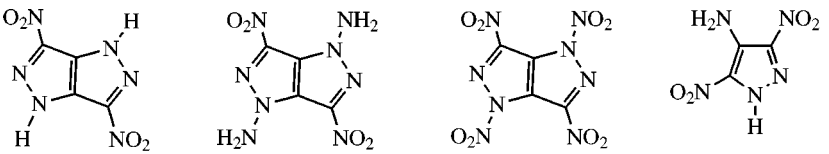

Figure 7 The molecules DNPP, LLM-119, LLM-121, and LLM-116.

by X-ray crystallography to be 1.865 g/cc (108). The crystal density is less than the density predicted by MOLPAK but agrees with the group additivity prediction. DNPP is a thermally stable [peak exotherm on differential scanning calorimetry (DSC) at 603 K] energetic material relatively insensitive to shock. The good thermal stability and performance of DNPP make this compound an attractive alternative to RDX, TATB, and TNT. DNPP has two acidic protons with $pK_a = 6$ and 3, respectively, that may be problematic in some applications.

DNPP was also used as a precursor to 1,4-diamino-3,6-dinitropyrazolo [4,3-c]pyrazole (LLM-119). N-amino derivatives of nitrohetrocycles, in comparison to the parent compounds, have an increased predicted performance and possess no acidic protons. LLM-119 was synthesized by amination of DNPP. LLM-119 has a density of 1.845 g/cc as determined by X-ray crystallography (108), which is significantly lower than predicted in Table 3. The low density may be attributed to the fact that the crystal structure shows the amino groups are orthogonal to the plane of the molecule. This is contrary to the predicted ab initio geometry, where the amino groups are in the same plane as the rest of the molecule. The ab initio geometry maximizes the delocalization of their lone pair of electrons with the heterocylic π–electron system and maximizes hydrogen bonding with the nitro groups. With the lower than anticipated density, LLM-119 has a predicted performance 90% that of HMX, based on the experimental density and predicted heat of formation. In this case, the underprediction of density led to a significant decrease in the expected performance of the material. LLM-119 has a peak exotherm at 526 K as determined by DSC; the thermal stability is good for an N-amino compound.

Efforts to synthesize the target materials with performance significantly greater than HMX have not been fully successful. Attempts at further nitration of DNPP to LLM-121 yielded a highly sensitive product. IR spectral analysis and ^{2}H-NMR suggest that LLM-121 is produced. LLM-121 is highly reactive and is itself an effective nitrating agent. LLM-121 may spontaneously revert to DNPP in most common solvents. It appears that very high-energy heterocycles are synthetically achievable but may not be sufficiently stable for routine handling.

Pagoria et al (109) reported the first use of 1,1,1-trimethylhydrazinium iodide (TMHI) as a nucleophilic aminating reagent in the amination of a series of 3-substituted nitrobenzenes. This method uses chemistry coined by Makosza & Winiarski (110) as the "vicarious nucleophilic substitution of hydrogen" in which an amino-group formally replaces a hydrogen atom on an electrophilic aromatic ring. Pagoria used this method to synthesize 4-amino-3,5-dinitropyrazole (LLM-116) (111). LLM-116 has a density of 1.90 g/cc (108), a decomposition point of 451 K, and is relatively insensitive to shock.

Pyrazines and Pyridines

The difficulty of synthesizing nitrated heteroaromatic systems can be attributed to their electron deficiency, making electrophilic aromatic substitution problematic. By the addition of electron-donating substituents to the heteroaromatic ring,

nitration may proceed more readily. This is illustrated in the next few examples in which activated pyridine and pyrazine precursors are nitrated to yield the desired dinitro-substituted heterocyles. These examples also illustrate the concept of increasing density and thermal stability by the use of an alternating array of amino- and nitro-groups.

Pagoria et al (107) reported the synthesis of 2,6-diamino-3,5-dinitropyrazine-1-oxide (LLM-105) by the oxidation of 2,6-diamino-3,5-dinitropyrazine (ANPZ) (112). LLM-105 has a density of 1.913 g/cc (108) and a decomposition point of 627 K. This work also illustrates another method to increase density and oxygen balance in heterocyclic systems, i.e., through the conversion of tertiary amines to their corresponding N-oxides. The N-O bond of a tertiary N-oxide is relatively strong, possessing significant double-bond character owing to π-back bonding by the lone pair of electrons of the oxygen (113). The formation of a heterocyclic N-oxide also changes the charge distribution of the heterocyclic ring and leads to, in some cases, an increase in the aromaticity of the heterocyclic ring, thus stabilizing the ring system (113). It should be noted that ANPZ has a crystal density of 1.84 g/cc (108), whereas LLM-105 has a crystal density of 1.913 g/cc. Thus the N-oxide functionality not only increases oxygen balance but also allows better crystal packing. Ritter & Licht (114) reported the synthesis of 2,6-diamino-3,5-dinitropyridine-1-oxide (ANPyO). ANPyO has a density of 1.878 g/cc and a melting point (mp) $>$ 613 K with decomposition (dec). Hollins et al (115, 116) extended this work and synthesized 2,4,6-triamino-3,5-dinitropyridine-1-oxide (compound 1) by the amination of ANPyO. Compound 1 is an insensitive energetic material with a density of 1.876 g/cc and a mp 581 K(dec) (see Figure 8).

Tetrazines

Coburn et al (117) reported the synthesis of 3,6-diamino-1,2,4,5-tetrazine-1,4-dioxide (LAX-112), an example of a cycloaromatic energetic material without a nitro-group as an oxidizing group. LAX-112 has a relatively high detonation velocity and good density. Using a more aggressive final oxidation step, 3-amino-6-nitro-1,2,4,5-tetrazine-2,4-dioxide was made, a sensitive, energetic material that decomposes at 383 K (117) (see Figure 9).

Chavez & Hiskey (118) have continued the research on 1,2,4,5-tetrazine-based explosives and synthesized a number of derivatives that are interesting as propellant

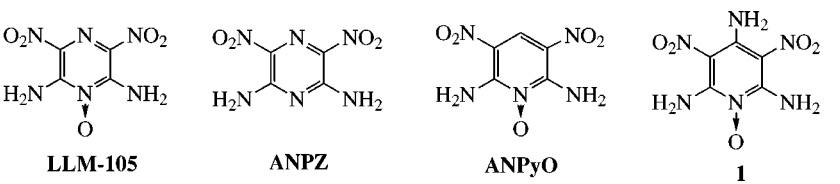

Figure 8 The molecules LLM-105, ANPZ, ANPyO, and compound 1.

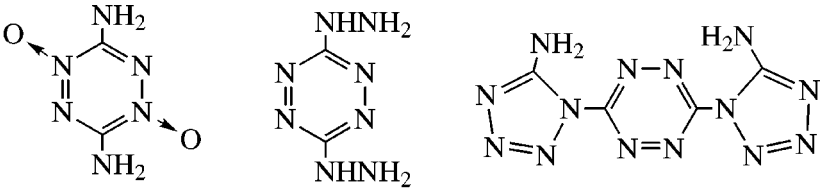

Figure 9 The molecules LAX-112, DHT, and compound 2.

and pyrotechnic ingredients because of their low carbon content. An example is 3,6-dihydrazino-1,2,4,5-tetrazine (DHT) (119), an energetic fuel with a density of 1.61 g/cc and a $\Delta H_f = 536$ kJ/mol. DHT was further converted to 3,6-bis (1H-1,2,3,4-tetrazol-5-ylamino)-1,2,4,5-tetrazine (2), which has a mp = 537 K and a measured $\Delta H_f = 883$ kJ/mol. Chavez and co-workers (120) recently reported the synthesis of 3,3′-azobis(6-amino-1,2,4,5-tetrazine (3), a high-nitrogen propellant ingredient with a density of 1.84 g/cc, a mp = 546 K, and a $\Delta H_f = +862$ KJ/mol (see Figure 10).

Furazans

3,4-Diaminofurazan (DAF), first synthesized by Coburn (121), has been an important precursor to a series of furazan-based energetic materials that are necessary as propellant ingredients and explosives. Solodyuk et al (122) reported the oxidation of DAF to yield 3-amino-4-nitrofurazan (ANF); 4,4′-diamino-3,3′-azoxyfurazan (DAAF); or 4,4′-diamino-3,3′-azofurazan (DAAzF). Chavez et al (120) scaled-up the synthesis of DAAF and performed measurements of its explosive properties. DAAF has a higher energy content than TATB. DAAF has a crystal density of 1.747 g/cc, a $\Delta H_f = 444$ kJ/mol, and is not sensitive to impact. Sheremetev and co-workers (123) have exploited the high reactivity of the nitro- groups of DNF, DNAF, and DNAzF to nucleophiles in the synthesis of a large number of 3-substituted-4-nitrofurazan derivatives (Figure 11).

Gunasekaran & Boyer (124) synthesized a highly energetic liquid [boiling point (bp) = 433–438 K], 5-[4-nitro-(1,2,5)oxadiazolyl]-5*H*-[1,2,3]triazolo[4,5-c][1,2,5]oxadiazole (NOTO) from DAAF.

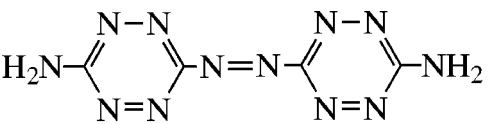

Figure 10 Compound 3.

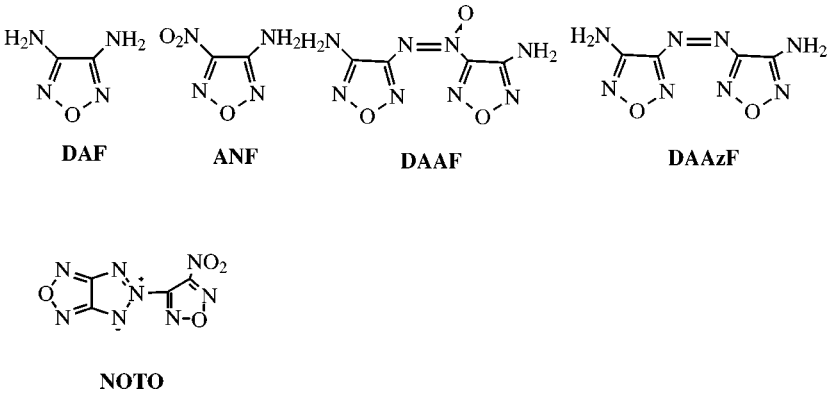

Figure 11 DAF, ANF, DAAF, DAAzF, and NOTO.

Trinitroazetidine (TNAZ) and Small-Ring Energetic Materials

Highly nitrated small-ring heterocycles and carbocycles are interesting energetic materials because of the increased performance from the additional energy release upon opening of the strained ring system during decomposition. The most widely studied small-ring energetic material to date is 1,1,3-trinitroazetidine (TNAZ), a melt-castable explosive. TNAZ has a mp of 376–377 K, a crystal density of 1.84 g/cc, and thermal stability >513 K. TNAZ was first synthesized by Archibald and co-workers (125). Coburn and co-workers (126) improved the synthesis, making it more amenable to scale-up. Other alternative synthetic pathways to TNAZ have been investigated (127, 128) (Figure 12).

Hiskey et al (129) have synthesized 3,3-dinitroazetidine (DNA), an energetic material with a pK_b of 6.5. They (129) exploited this basicity and synthesized a number of energetic salts. All these salts have low differential thermal analysis (DTA) exotherms (413–433 K) and impact sensitivities ranging from sensitive to moderately sensitive.

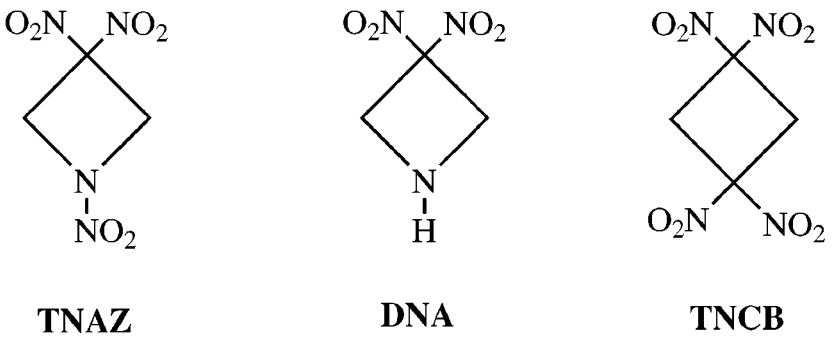

Figure 12 TNAZ, DNA, and TNCB.

Earlier, Archibald et al reported the synthesis of 1,1,3,3-tetranitrocyclobutane (TNCB) (130) by the oxidative nitration of 1,3-dinitrocyclobutane with $AgNO_3$ and $NaNO_2$. TNCB has a crystal density = 1.83 g/cc and a mp = 438 K.

Nitrotriazoles

The synthesis of nitrotriazoles as energetic materials and as intermediates to energetic materials has received a great deal of attention in the past ten years (131). The most studied nitrotriazole explosive, 4,6-bis(5-amino-3-nitro-1,2,4-triazolyl)-5-nitropyrimidine (DANTNP), was reported by Wartenberg and co-workers (132). The conception and synthesis of DANTNP is an example of models guiding the synthesis of new energetic materials. Sensitivity prediction was performed by the method of Delpuech et al (62). DANTNP is an insensitive explosive with a crystal density of 1.865 g/cc, $\Delta H_f = 431$ kJ/mol, mp = 603 K, and performance similar to TATB (Figure 13).

3-Nitro-5-amino-1,2,4-triazole (ANTA) was first prepared by Pevzner et al (133). Lee and co-workers (134) subsequently reported an improved synthesis of ANTA. Simpson et al (135) used this method of synthesis, with some small modifications, to scale-up the synthesis of ANTA. ANTA was found to be an insensitive energetic material with a density of 1.819 g/cc, $\Delta H_f = 88$ kJ/mol, a mp = 511 K, and performance similar to TATB.

Ammonium Dinitramide

Bottaro et al (136) reported in 1991 the synthesis of ammonium dinitramide (ADN) $[(NH_4)^+ N(NO_2)_2^-]$. ADN is a very strong oxidizer that may have potential uses in environmentally benign rocket propellant ingredient and as a cationic phase transfer agent. Following this paper, Tartakovsky et al (137–143) published a number of articles on their research on the synthesis and use of dinitramide salts. A significant number of salts of the dinitramide anion have been synthesized, including the alkali salts and the guanidinium; hydroxylammonium; aminoguanidinium; cubane-1,4-diammonium; cubane-1,2,4,7-tetraammonium; biguanidinium; and 1,2-ethylenediammonium salts (136).

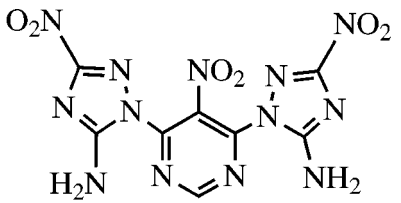

DANTNP

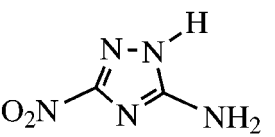

ANTA

Figure 13 DANTNP and ANTA.

ADN is a very strong acid with a $pK_a \sim -5$, is stable between pH 0–15, but slowly decomposes in concentrated acid. It has a mp = 365 K and a DTA exotherm that leaves the baseline at 403 K and peaks at 669 K, and a density of 1.801 g/cc (144).

Highly Nitrated Cage Compounds

Highly nitrated cage compounds hold great promise as energetic materials, based on the premise that the strained rings of cage compounds and the rigid, highly compact cage structure should result in a highly dense, more powerful explosive. A drawback has been the corresponding increase in the difficulty in synthesis of these caged structures. The most studied example of highly nitrated cage compounds is 2,4,6,8,10,12-hexanitro-2,4,6,8,10,12-hexaazatetracyclo[5.5.0.05.9.03,11]dodecane (CL-20), first synthesized by Nielsen and co-workers (145) at the Naval Air Warfare Center-China Lake. CL-20 (see Figure 14) is the most powerful explosive currently being investigated at the pilot plant scale or larger (146). CL-20, in its ε-crystal polymorph, has a density of 2.04 g/cc and a DSC decomposition temperature of 501 K.

Highly nitrated cubanes and azacubanes were predicted to be very dense, highly energetic compounds with explosive performance greater than CL-20 (147–152) (see Figure 14). Recently Zhang and co-workers (153) reported the synthesis of heptanitrocubane (compound 4) and octanitrocubane (compound 5), the culmination of an ongoing project in the synthesis of nitrocubanes as energetic materials. Previously, Eaton et al (154) reported the synthesis of 1,3,5,7-tetranitrocubane (compound 6) from the oxidation of the tetramino derivative with dimethyldioxirane. Tetranitrocubane has a density of 1.814 g/cc and a mp = 475 K. The more highly nitrated species proved to be more difficult to synthesize. The pentanitro- (ρ = 1.959 g/cc) and hexanitrocubanes (155) were synthesized by the treatment of the anion of tetranitrocubane with N_2O_4 at the interface between frozen THF and N_2O_4. Heptanitrocubane was synthesized by the treatment of tetranitrocubane with $NaN(TMS)_2$ and frozen N_2O_4 in THF/isopentane. Octanitrocubane was synthesized by the treatment of heptanitrocubane with $LiN(TMS)_2$ in CH_2Cl_2 at 195 K

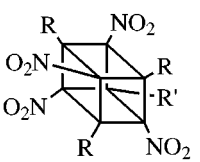

4, R=NO_2, R'=H
5, R=R'=NO_2
6, R=R'=H

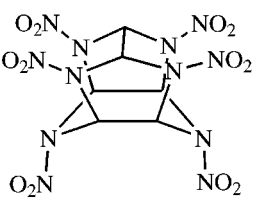

CL-20

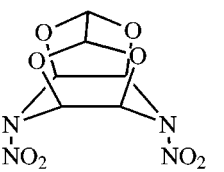

7

Figure 14 Compounds 4–7 and CL-20.

with NOCl followed by ozonation. Heptanitrocubane has a density of 2.028 g/cc whereas octanitrocubane has a density of 1.979 g/cc (Figure 14).

Vayalakkavoor and co-workers (156) reported the synthesis of 4,10-dinitro-2,6,8,12-teraoxo-4,10-diazatetracyclo[5.5.0.05,9.03,11]dodecane (7) (Figure 14). Compound 7 has the surprisingly high density of 1.99 g/cc, considering it possesses only two nitramine moieties. The high density was attributed to the caged structure. It is thermally stable with an mp > 523 K and has been investigated as an insensitive energetic material.

Polynitrogen Compounds

Polynitrogen compounds are of significant interest as high-energy density materials (see above). Recently, Christe and co-workers (157) synthesized $N_5^+AsF_6^-$, the first example of a new homoleptic polynitrogen ion since the discovery of the azide ion in 1890. $N_5^+AsF_6^-$ was synthesized by the condensation of $N_2F^+AsF_6^-$ with HN_3 at 195 K in anhydrous HF. $N_5^+AsF_6^-$ is a white solid that is marginally stable at room temperature but can be stored for weeks at 195 K.

Nanostructured Energetic Materials

Alternative approaches to monomolecular energetic materials have been formulations of separate fuels and oxidizers. These composites have the potential for significantly greater energy density, but energy release rates have been dramatically slower than monomolecular counterparts owing to mass transport rates. Recent developments have reduced the scale of mixing to the nanometer range. Aumann et al (158) developed a gas condensation method to produce 20–40 nm particles of MoO_3 and passivated Al. When stoichiometrically mixed, an energy density greater than 16 kJ/cm^3 can be attained. Very fast burn rates have been reached, making these nanostructured materials attractive alternatives to monomolecular structures. Other methods to prepare energetic nanostructures include chemical syntheses and epitaxial deposition. One technique uses sol-gel chemistry to produce nanometer scale gels made of either a fuel or oxidizer (159, 160). Both organic and inorganic gels may be made. Figure 15 shows a Fe_2O_3 gel (the oxidizer) with 30-nm aluminum particles (the fuel) entrained. The primary particle cluster sizes are 2 to 5 nm. For all these nanostructured materials there are few property data, and the effect on reactivity of increased surface area, high surface energy, and higher compressive stresses in nanoparticles is largely unknown.

CONCLUSION

The design of energetic materials is currently in a transitional stage. While certain properties can be predicted with confidence, others elude current simulation methods. Thermochemical calculations of energetic material energy delivery are probably the most mature. Detonation properties of mixtures of known compounds

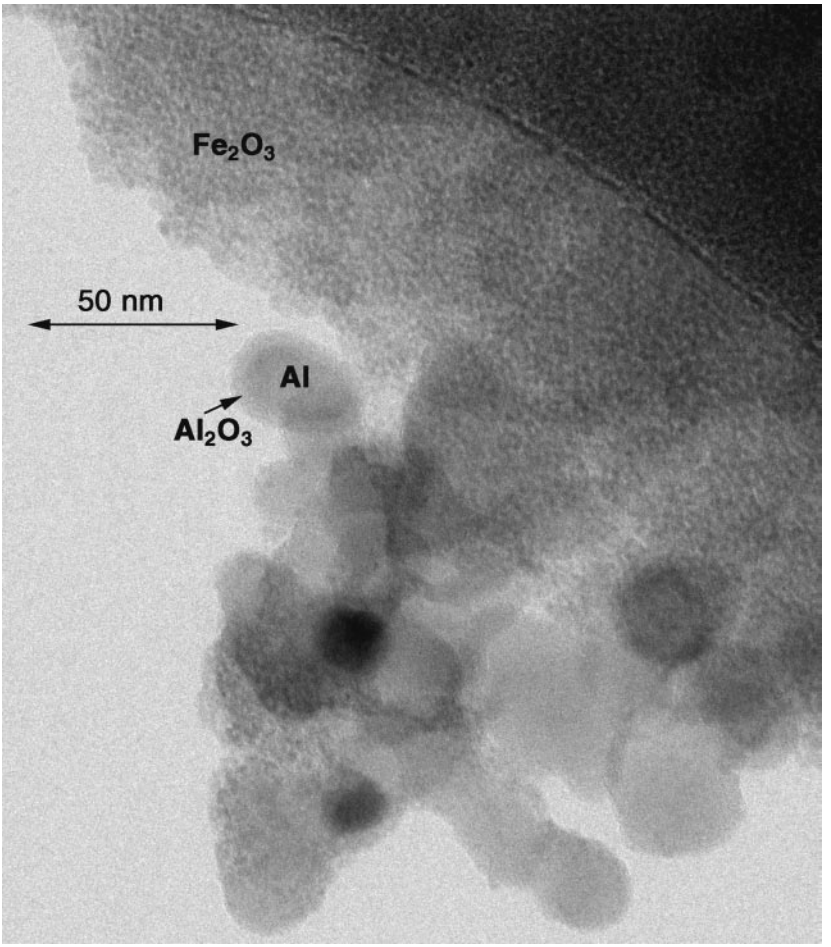

Figure 15 LA Fe_2O_3 gel (the oxidizer) with 30-nm aluminum particles (the fuel) entrained.

can be calculated with errors of roughly 2–3%. Higher uncertainties occur, however, with composite materials including high concentrations of metals and other slowly reacting components. In this case, the development of kinetic detonation schemes shows promise for the future.

Significant progress has been made in the last several years in the prediction of the gas phase heat of formation. The calculation of the solid phase heat of formation, however, is less well developed. The lattice energy now represents the greatest uncertainty in estimating the energy content of molecular solids. Density prediction schemes are not yet mature. Although several atomistic methods have been developed, group additivity is also a competitive practical method. The prediction of energetic material stability is hindered by a lack of basic theoretical

understanding. Simply calculating the bond dissociation of an isolated molecule may provide some insight, given that the molecular energy content is also taken into account.

The above uncertainties in the design of energetic materials can lead researchers into inadvertently overestimating material stability and performance. The overestimation is produced by simple selection; researchers select from a large set of candidates, i.e., those materials with the most outstanding predicted properties. Sometimes, however, what is selected is merely a molecule poorly treated by the computational method. The development of more robust performance and stability predicting tools will help to alleviate this difficulty.

Synthesis of new energetic materials with novel combinations of properties is continuing to proceed at a rapid pace. Most of these materials, however, live within a rough envelope of tradeoffs between energy and stability. New material classes, such as nano-compositie materials, may offer tradeoffs that are more favorable. More sophisticated synthetic techniques can optimize the tradeoff between energy and stability but usually at an increased material cost. The importance of material cost diminishes, however, as energetic materials find new, technically sophisticated, applications. In the future, we expect a wider range of energetic materials to be tailored to specific applications.

ACKNOWLEDGMENTS

This work was performed under the auspices of the US Department of Energy by the Lawrence Livermore National Laboratory under contract No. W-7405-ENG-48.

LITERATURE CITED

1. Fickett W, Davis WC. 1979. *Detonation*. Berkeley: Univ. Calif. Press
2. Lommerse JPM, Motherwell WDS, Ammon HL, Dunitz JD, Gavezzotti A, et al. 2000. *Acta Crystall. B* 56:697–714
3. Tarver CM. 1979. *J. Chem. Eng. Data* 24:136
4. Stine JR. 1981. *A method for predicting the density of organic molecular crystals. Rep. LA8920*, Los Alamos, NM: Los Alamos Sci. Lab.
5. Ammon HL, Mitchell S. 1998. *Propellants Explosives Pyrotechnics* 23:260–65
6. Karfunkel HR, Gdanitz RJ. 1992. *J. Comput. Chem.* 13:1171–83
7. Holden JR, Du ZY, Ammon HL. 1993. *J. Comput. Chem.* 14:422–37
8. Piacenza G, Legsai G, Blaive B, Gallo R. 1996. *J. Phys. Org. Chem.* 9:427–32
9. Dzyabchenko AV, Pivina TS, Arnautova EA. 1996. *J. Mol. Struct.* 378:67–82
10. Sorescu DC, Rice BM, Thompson DL. 1999. *J. Phys. Chem. A* 103:989–98
11. Rice BM, Pai SV, Hare J. 1999. *Combustion Flame* 118:445–58
12. Habibollahzadeh D, Grice ME, Concha MC, Murray JS, Politzer P. 1995. *J. Comput. Chem.* 16:654–58
13. Politzer P, Murray JS, Grice ME, Desalvo M, Miller E. 1997. *Mol. Phys.* 91:923–28

14. Fried LE, Souers PC. 1996. *Propellants, Explosives, Pyrotechnics* 21:215–23
15. Kistiakowsky GB, Wilson EB. 1941. *Report on the prediction of detonation velocities of solid explosives. Rep. OSRD-69*, Washington, DC: Off. Sci. Res. Dev.
16. Finger M, Lee E, Helm FH, Hayes B, Hornig H, et al. 1976. *The effect of elemental composition on the detonation behavior of explosives*. Sixth Int. Symp. Detonation, Coronado, CA
17. Mader CL. 1979. *Numerical Modeling of Detonations*. Berkeley, CA: Univ. Calif. Press
18. Gubin SA, Odintsov VV, Pepekin VI. 1985. *Sov. J. Chem. Phys.* 3:1152
19. Hobbs ML, Baer MR. 1993. *Calibrating the BKW-EOS with a large product species data based and measured C-J properties*. Tenth Int. Detonation Symp., Boston, MA
20. Souers PC, Kury JW. 1993. *Propellants, Explosives, Pyrotechnics* 18:175
21. Cowperthwaite M, Zwisler WH. 1976. *The JCZ equation of state for detonation products and their incorporation into the TIGER code*. Sixth Int. Symp. Detonation Coronado, CA
22. Hobbs ML, Baer MR, McGee BC. 1999. *Propellants, Explosives, Pyrotechnics* 24:269–79
23. Deleted in proof
24. Ross M. 1979. *J. Chem. Phys.* 71:1567
25. Ross M, Ree FH. 1980. *J. Chem. Phys.* 73:6146–52
26. Ree FH. 1984. *J. Chem. Phys.* 81:1251
27. van Thiel M, Ree FH. 1987. *J. Appl. Phys.* 62:1761–67
28. van Thiel M, Ree FH. 1996. *J. Chem. Phys.* 104:5019–25
29. Kang HS, Lee CS, Ree T, Ree FH. 1985. *J. Chem. Phys.* 82:414
30. Byers Brown W. 1987. *J. Chem. Phys.* 87:566
31. Charlet F, Turkel ML, Danel JF, Kazandjian L. 1998. *J. Appl. Phys.* 84:4227–38
32. Fried LE, Howard WM. 1998. *J. Chem. Phys.* 109:7338–48
33. Ree FH. 1986. *J. Chem. Phys.* 84:5845–56
34. Fried LE, Howard WM. 1999. *J. Chem. Phys.* 110:12023–32
35. Shaw MS. 1991. *J. Chem. Phys.* 94:7550–53
36. Leland TW, Rowlinson JS, Sather GA. 1947. *Trans. Faraday Soc.* 64:1447
37. Kerley GI. 1985. *Theoretical equations of state for the detonation products of explosives*. Eighth Int. Symp. Detonation, Albuquerque, NM
38. Reed TM, Gubbins KE. 1973. *Statistical Mechanics*. New York: McGraw-Hill
39. Jones HD, Zerilli FJ. 1991. *J. Appl. Phys.* 69:3893–900
40. van Thiel M, Ree FH. 1989. *Int. J. Thermophys.* 10:227–36
41. Fried LE, Howard WM. 2000. *Phys. Rev. B* 61:8734–43
42. Shaw MS, Johnson JD. 1987. *J. Appl. Phys.* 62:2080–85
43. Viecelli JA, Ree FH. 1999. *J. Appl. Phys.* 86:237–48
44. Viecelli JA, Ree FH. 2000. *J. Appl. Phys.* 88:683–90
45. Wood WW, Kirkwood JG. 1954. *J. Chem. Phys.* 22:1920–24
46. Bdzil JB. 1981. *J. Fluid Mech.* 108:195–206
47. Stewart DS, Yao J. 1998. *Combustion Flame* 113:224–35
48. Howard WM, Fried LE, Souers PC. 1998. *Kinetic modeling of non-ideal explosives with Cheetah*. 11th Int. Symp. Detonation, Snowmass, CO
49. Fried LE, Howard WM, Souers PC. 1998. *Cheetah 2.0 User's Manual. Rep. UCRL-MA-117541 Rev. 5*, Livermore, CA: Lawrence Livermore Natl. Lab.
50. Murnaghan FD. 1944. *Proc. Natl. Acad. Sci. USA* 30:244–47
51. Seidel ET, Schaefer HF. 1988. *J. Chem. Phys.* 88:7043–49
52. Kim KS, Jang JH, Kim S, Mhin B, Schaefer HF. 1990. *J. Chem. Phys.* 92:1887–92
53. Lee TJ, Rice JE. 1991. *J. Chem. Phys.* 94:1215–21

54. Engelke R, Stine JR. 1990. *J. Phys. Chem.* 94:5689–94
55. Brill TB, James KB. 1993. *J. Phys. Chem.* 97:8752–58
56. Dlott DD. 1999. *Annu. Rev. Phys. Chem.* 50:251–78
57. Dlott DD, Fayer MD. 1990. *J. Chem. Phys.* 92:3798–812
58. Fried LE, Ruggiero AJ. 1994. *J. Phys. Chem.* 98:9786–91
59. Coffey CS. 1993. *Energy localization and the initiation of explosive crystals by shock or impact*. Structure and Properties of Energetic Materials, Boston, MA
60. Williams F. 1971. *Adv. Chem. Phys.* 21:289–302
61. Dremin AN, Klimenko VY, Davidova ON, Zoludeva TA. 1989. *Multiprocess detonation model*. Ninth Int. Symp. Detonation, Portland, OR
62. Delpuech A, Cherville J, Michaud C. 1981. *Molecular electronic structure and initiation of secondary explosives*. Seventh Int. Symp. Detonation, Annapolis, MD
63. Sharma J. 1991. In *Shock Compression of Condensed Matter*, ed. SC Schmidt, RD Dick, JW Forbes, DG Tasker. Williamsburg VA: Elsevier
64. Sharma J, Beard BC, Chaykovsky M. 1991. *J. Phys. Chem.* 95:1209–13
65. Gilman JJ. 1995. *Philos. Mag. B* 71:1057–68
66. Kuklja MM, Stefanovich EV, Kunz AB. 2000. *J. Chem. Phys.* 112:3417–23
67. Manaa MR, Fried LE. 1999. *J. Phys. Chem. A* 103:9349–54
68. Takezaki M, Hirota N, Terazima M. 1997. *J. Phys. Chem. A* 101:3443–48
69. Rajchenbac C, Gediminas J, Rulliere C. 1995. *Chem. Phys. Lett.* 231:467–75
70. Reed EJ, Joannopoulos JD, Fried LE. 2000. *Phys. Rev. B* 62:16500–9
71. Shaw R, Decarli PS, Ross DS, Lee EL, Stromberg HD. 1979. *Combustion Flame* 35:237
72. Shaw R, Decarli PS, Ross DS, Lee EL, Stromberg HD. 1983. *Combustion Flame* 50:123
73. Engelke R, Schiferl D, Storm CB, Earl WL. 1988. *J. Phys. Chem.* 92:6815
74. Brasch JW. 1980. *J. Phys. Chem.* 84:2084
75. Naud DL, Brower KR. 1992. *High-Pressure Res.* 11:65
76. Blais NC, Engelke R, Sheffield SA. 1997. *J. Phys. Chem. A* 101:8285–95
77. Winey JM, Gupta YM. 1997. *J. Phys. Chem. B* 101:10733–43
78. Winey JM, Gupta YM. 1997. *J. Phys. Chem. A* 101:9333–40
79. Gruzdkov YA, Gupta YM. 1998. *J. Phys. Chem. A* 102:2322–31
80. Kress JD, Bickham SR, Collins LA, Holian BL, Goedecker S. 1999. *Phys. Rev. Lett.* 83:3896
81. Bickham SR, Kress JD, Collins LA. 2000. *J. Chem. Phys.* 112:9695
82. Politzer P, Murray JS. 1996. *J. Mol. Struct.* 376:419
83. Wu CJ, Fried LE. 1998. *First principles study of decomposition energetics*. Proceed. 11th Int. Symp. Detonation, Snowmass, CO
84. Dobratz BM, Crawford PC. 1985. *LLNL Explosives Handbook*. Rep. UCRL-52997
85. Hall TN, Holden JR. 1985. *Navy Explosives Handbook: Explosion Effects and Properties Part III. Rep. NSWC MP88–116*, Dahlgren, VA: Naval Surface Warfare Center
86. Kohler J, Meyer R. 1993. *Explosives*. Weinheim, Germany: VCH
87. Christe KO, Wilson WW, Sheehy JA, Boatz JA. 1999. *Ang. Chem. Int. Ed.* 38:2004–9
88. Reichlin R, Schiferl D, Martin S, Vanderborgh C, Mills RL. 1985. *Phys. Rev.Lett.* 55:1464
89. Bell PM, Mao HK, Hemley RJ. 1986. *Physica B* 139:16
89a. Goncharov AF, Gregoryanz E, Mao H, Zhenxian L, Hemley RJ. 2000. *Phys. Rev. Lett.* 85:1262

90. McMahan AK, LeSar R. 1985. *Phys. Rev. Lett.* 54:1929
91. Martin RM, Needs RJ. 1986. *Phys. Rev. B* 34:5082
92. Mailhiot C, Yang LH, McMahan AK. 1992. *Phys. Rev. B* 46:14419
93. Radousky HB, Nellis WJ, Ross M, Hamilton DC, Mitchell AC. 1986. *Phys. Rev. Lett.* 57:2419
94. Ross M. 1987. *J. Chem. Phys.* 86:7110
95. Lauderdale WJ, Stanton JF, Bartlett RJ. 1992. *J. Phys. Chem.* 96:1173
96. Leininger ML, Sherrill CD, Schaefer HF. 1995. *J. Phys. Chem.* 99:2324
97. Glukhovtsev MN, Schleyer PR. 1993. *Int. J. Quantum Chem.* 46:119
98. Dunn KM, Morokuma KJ. 1995. *J. Chem. Phys.* 102:4904
99. Alkorta I, Elguero J, Rozas I, Balaban AT. 1990. *J. Mol. Struct.* 206:67
100. Engelke R. 1993. *J. Am. Chem. Soc.* 115:2961
101. Tian A, Ding F, Zhang L, Xie Y, Schaefer HF. 1997. *J. Phys. Chem. A* 101:1946
102. Leininger ML, Huis TJV, Schaefer HF. 1997. *J. Phys. Chem. A* 101:4460
103. Gagliardi L, Evangelisti S, Roos BO, Widmark P. 1998. *J. Mol. Struct.* 428:1
104. Manaa MR. 2000. *Chem. Phys. Lett.* 331:262–68
105. Agrawal JP. 1998. *Prog. Energy Combustion Sci.* 24:1–30
106. Shevelev SA, Dalinger IL, Shkineva TK, Ugrak BI, Gulevskaya VI, Kanishchev MI. 1993. *Russ. Chem. Bull.* 42:1063–68
107. Pagoria PF, Mitchell AR, Schmidt RD, Simpson RL, Garcia F, et al. 1998. *Synthesis, scale-up and experimental testing of LLM-105* (*2,6–diamino-3,5–dinitropyrazine-1–oxide*). Insensitive Munitions and Energetic Materials Technology Symp., Meet. No. 956, San Diego, CA
108. Gilardi R. 2000. *X-ray crystallographic determination*. Washington, DC: Naval Res. Lab.
109. Pagoria PF, Mitchell AR, Schmidt RD. 1996. *J. Organic Chem.* 61:2934–35
110. Makosza M, Winiarski J. 1987. *Acc. Chem. Res.* 20:282–89
111. Pagoria PF, Mitchell AR, Schmidt RD. 1996. *Vicarious amination of nitroarenes with trimethylhydrazinium iodide*. 211th Am. Chem. Soc. Natl. Meet. New Orleans, LA
112. Donald DS. 1974. *U.S. Patent No. 3,808,209*
113. Albini A, Pietra S. 1991. *Heterocyclic-N-oxides*. Boca Raton, FL: CRC Press
114. Ritter H, Licht HH. 1995. *J. Heterocyclic Chem.* 32:585–90
115. Hollins RA, Merwin LH, Nissan RA, Wilson WS, Gilardi R. 1996. *J. Heterocyclic Chem.* 33:895–904
116. Hollins RA, Merwin LM, Nissan RA, Wilson WW, Gilardi R. 1996. *Aminonitroheterocyclic-N-oxides–a new class of insensitive energetic materials*, pp. 31-36. Pittsburgh, PA: Mater. Res. Soc. Symp.
117. Coburn MD, Hiskey MA, Lee KY, Ott DG, Stinecipher MM. 1993. *J. Heterocyclic Chem.* 30:1593–95
118. Chavez DE, Hiskey MA. 1999. *J. Energetic Mater.* 17:357–77
119. Chavez DE, Hiskey MA. 1998. *J. Heterocyclic Chem.* 35:1329–32
120. Chavez D, Hill L. Hiskey M, Kinkead S. 2000. *J. Energetic Mater.* 18:219–36
121. Coburn MD. 1968. *J. Heterocyclic Chem.* 5:83–87
122. Solodyuk GD, Boldyrev MD, Gidaspov BV, Nikolaev VD. 1981. *J. Organic Chem. USSR* (*Engl.*) 17:756–59
123. Sheremetev AB, Kharitonova OV, Mantseva EV, Kulagina VO, Shatunova EV, et al. 1999. *Z. Organic. Khimii* 35:1555–66
124. Gunasekaran A, Boyer JH. 1993. *Heteroatom Chem.* 4:521–24
125. Archibald TG, Gilardi R, Baum K, George C. 1990. *J. Organic Chem.* 55:2920–24

126. Coburn MD, Hiskey MA, Archibald TG. 1997. *Waste Management* 17:143–46
127. Hayashi K, Kumagai T, Nagao Y. 2000. *Heterocycles* 53:447–52
128. Marchand AP, Rajagopal D, Bott SG, Archibald TG. 1995. *J. Organic Chem.* 60:4943–46
129. Hiskey MA, Coburn MD, Mitchell MA, Benicewicz BC. 1992. *J. Heterocyclic Chem.* 29:1855–56
130. Archibald TG, Garver LC, Baum K, Cohen MC. 1989. *J. Organic Chem.* 54:2869–73
131. Yuxiang O, Boren C, Jiarong L, Shuan D, Jianjuan L, Huiping J. 1994. *Heterocycles* 38:1651–64
132. Wartenberg C, Charrue P, Laval F. 1995. *Propellants Explosives Pyrotechnics* 20:23–26
133. Pevzner MS, Kulibabina TN, Povarova NA, Kilina LV. 1979. *Khim. Geterotskil* 8:1132–35
134. Lee KY, Storm CB, Hiskey MA, Coburn MD. 1991. *J. Energetic Mater.* 9:415–28
135. Simpson RL, Pagoria PF, Mitchell AR, Coon CL. 1994. *Propellants Explosives Pyrotechnics* 19:174–79
136. Bottaro JC, Penwell PE, Schmitt RJ. 1997. *J. Am. Chem. Soc.* 119:9405–10
137. Lukyanov OA, Gorelik VP, Tatakovsky VA. 1994. *Russ. Chem. Bull.* 43:89–92
138. Lukyanov OA, Konnova YV, Klimova TA, Tartakovsky VA. 1994. *Russ. Chem. Bull.* 43:1200–2
139. Lukyanov OA, Anikin OV, Gorelik VP, Tartakovsky VA. 1994. *Russ. Chem. Bull.* 43:1457–61
140. Shlyapochnikov VA, Cherskaya NO, Lukyanov OA, Gorelik VP, Tartakovsky VA. 1994. *Russ. Chem. Bull.* 43:1522–25
141. Shlyapochnikov VA, Oleneva GI, Cherskaya NO, Lukyanov OA, Gorelik VP, et al. 1995. *Russ. Chem. Bull.* 44:1449–53
142. Lukyanov OA, Shlykova NI, Tartakovsky VA. 1994. *Russ. Chem. Bull.* 43:1680–83
143. Lukyanov OA, Agevnin AR, Leichenko AA, Seregina NM, Tartakovsky VA. 1995. *Russ. Chem. Bull.* 44:108–12
144. Martin A, Pinkerton AA, Gilardi RD, Bottaro JC. 1997. *Acta Crystall. B* 53:504–12
145. Nielsen AT, Chafin AP, Christian SL, Moore DW, Nadler MP, et al. 1998. *Tetrahedron* 54:11793–812
146. Simpson RL, Urtiew PA, Ornellas DL, Moody GL, Scribner KJ, Hoffman DM. 1997. *Propellants Explosives Pyrotechnics* 22:249–55
147. Reed LH, Jayasuria K, Koovaakat SK, Allen LC. 1991. *J. Phys. Org. Chem.* 4:714–20
148. Chapman DA, Kaufman JJ, Buenker RJ. 1991. *Int. J. Quantum Chem.* 40:389–403
149. Eremenko LT. 1997. *Chem. Phys. Rep.* 16:1675–83
150. Astakhov AM, Stepanov RS, Babushkin AY. 1998. *Combustion, Explosion, Shock Waves* 34:85–87
151. Kortus J, Pederson MR, Richardson SL. 2000. *Chem. Phys. Lett.* 332:224–30
152. Jursic BS. 2000. *J. Mol. Struct. Theochem.* 530:21–30
153. Zhang MX, Eaton PE, Gilardi R. 2000. *Ang. Chemie Int. Ed.* 39:401–4
154. Eaton PE, Xiong YS, Gilardi R. 1993. *J. Am. Chem. Soc.* 115:10195–202
155. Lukin KA, Li JC, Eaton PE, Kanomata N, Hain J, et al. 1997. *J. Am. Chem. Soc.* 119:9591–602
156. Vayalakkavoor RT, Vedachalam M, Boyer JH. 1990. *Heterocycles* 31:479–80
157. Christe KO, Wilson WW, Sheehy JA, Boatz JA. 1999. *Ang. Chemie. Int. Ed.* 38:2004–9
158. Aumann CE, Skofronick GL, Martin JA. 1995. *J. Vac. Sci. Technol. B* 13:1178–83
159. Tillotson TM, Hrubesh LW, Simpson RL, Lee RS, Swansiger RW, Simpson RL. 1998. *J. Non-Cryst. Solids* 225:358–63
160. Tillotson TM, Simpson RL, Hrubesh LW, Gash AE, Thomas IM, Poco JF. 2001. *J. Non-Cryst. Solids.* In press

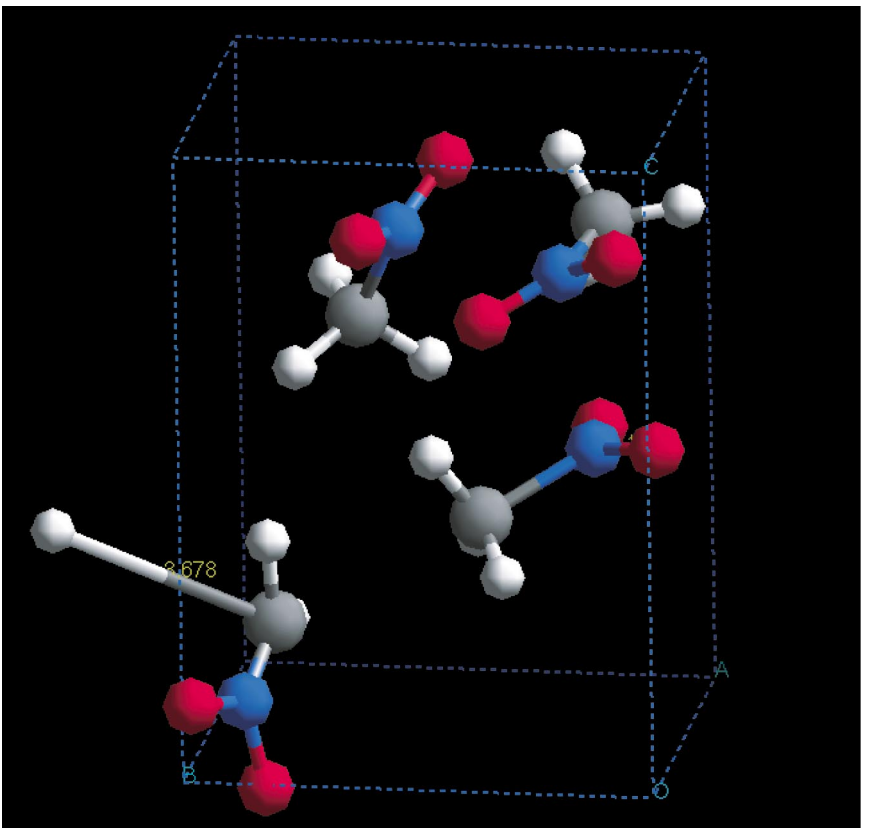

Figure 4 A snapshot of hydrogen abstraction in dissociating nitromethane after 200 fs at a density of 1.5 g/cm^3 and temperature of 3000 K. Carbon atoms are gray, nitrogen atoms are blue, oxygen atoms are red, and hydrogen atoms are white.

Annual Review of Materials Research
Volume 31, 2001

CONTENTS